JOC The Journal of Organic Chemistry

Article

pubs.acs.org/joc

Theoretical Foundation for the Presence of Oxacarbenium Ions in Chemical Glycoside Synthesis

Takashi Hosoya,*[,†] Toshiyuki Takano,[‡] Paul Kosma,[†] and Thomas Rosenau[†]

[†]Department of Chemistry, University of Natural Resources and Life Sciences, Muthgasse 18, A-1190 Vienna, Austria

[‡]Graduate School of Agriculture, Kyoto University, Kitashirakawaoiwake-cho, Sakyoku, Kyoto-shi, Kyoto 606-8502, Japan

Supporting Information

ABSTRACT: Glycoside formation in organic synthesis is believed to occur along a reaction path involving an activated glycosyl donor with a covalent bond between the glycosyl moiety and the leaving group, followed by formation of contact ion pairs with the glycosyl moiety loosely bound to the leaving group, and eventually solvent-separated ion pairs with the glycosyl moiety and the leaving group being separated by solvent molecules. However, these ion pairs have never been experimentally observed. This study investigates the formation of the ion pairs from a covalent intermediate, 2,3,4,6-tetra-*O*-methyl-α-D-glucopyranosyl triflate, by means of computational chemistry. Geometry optimization of the ion pairs without solvent molecules resulted in re-formation of the covalent α- and β-triflates but was successful when four solvent (dichloromethane) molecules were taken into account. The DFT(M06-2X) computations indicated interconversion between the α- and β-covalent intermediates via the α- and β-contact ion pairs and the solvent-separated ion pairs. The calculated activation Gibbs energy of this interconversion was quite small (10.4−13.5 kcal/mol). Conformational analyses of the ion pairs indicated that the oxacarbenium ion adopts $^{4}H_{3}$, $^{2}H_{3}/E_{3}$, $^{2}H_{3}/^{2}S_{0}$, E_{3}, $^{2,5}B$, and $B_{2,5}$ pyranosyl ring conformations, with the stability of the conformers being strongly dependent on the relative location of the counteranion.

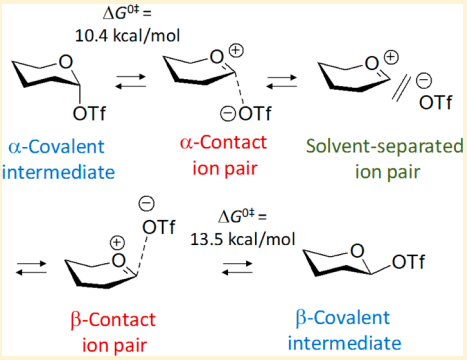

INTRODUCTION

Synthesis of glycosidic bonds is one of the major research fields in organic chemistry as well as carbohydrate chemistry.[1,2] Knowledge of the detailed reaction mechanisms in glycoside synthesis will be highly beneficial for synthesizing glycosidic bonds in more efficient ways, e.g. achieving higher α/β stereoselectivity. To this end, researchers have been making efforts to understand the reaction in a more systematic way.[1b,c,3−14] A wide range of investigations have been carried out especially for glycosyl triflate donors, which are intermediately generated as the actual glycosyl donors.[1b,c,4−10] As shown in Scheme 1 (L = TfO), activation of the starting material, e.g. glycosyl sulfoxides by Tf_2O, results in formation of an equilibrium mixture of α- and β-covalent intermediates that each have a covalent bond between the TfO group and the glycosyl moiety. These bonds involve α- and β-configured contact ion pairs with the TfO group and the glycosyl moiety loosely bound by electrostatic interaction. The cationic glycosyl moiety and TfO^{-} anion become solvent-separated ion pairs. The covalent intermediates and the contact ion pairs react with acceptor alcohols according to S_N2-like mechanisms, while the solvent-separated ion pairs react according to S_N1 pathways.[1] Because these S_N1- and S_N2-like reactions are simultaneous, both α- and β-glycosides are obtained as the final products with their ratio being determined by different contributing factors.

Although the mechanisms in Scheme 1 are frequently mentioned in mechanistic discussions on glycoside synthesis, detailed information about the components of the equilibrium, especially that about the ion pairs, is limited.[15] This is mainly due to the fact that the covalent intermediates and the ion pairs are too unstable to be directly detectable. Low-temperature NMR experiments, for instance, allow observation of the α-covalent intermediate, which is usually the most stable in the equilibrium mixture, but fail to provide information about the other chemical species in Scheme 1.[8,10] Several studies reported that the oxacarbenium ion was observed in mass spectrometric analysis of glycosyl donors,[16] but the high-vacuum conditions employed were not necessarily relevant to the solvated conditions in glycoside synthesis.

Quantum chemical calculations have also been applied for elucidating the occurrence of the equilibrium as well as the reactivity of the oxacarbenium ions;[5,17−25] as such, computational investigations potentially provide detailed information about unstable intermediates and transition states. However, the contact ion pairs and the solvent-separated ion pairs are usually not obtained as equilibrium species in geometry optimization unless the system is artificially modified. For example, the ion pairs are only obtained as equilibrium species when a lithium cation is embedded close to the leaving group anion to avoid accumulation of negative charge on the leaving group.[18] Due to this failure of the geometry optimization,

Received: May 9, 2014
Published: August 8, 2014

dx.doi.org/10.1021/jo501012s | J. Org. Chem. 2014, 79, 7889−7894

Scheme 1. Equilibrium among Covalent Intermediates, Contact Ion Pairs (CIPs), and Solvent-Separated Ion Pairs (SSIPs) and Their Glycosylation Reactions

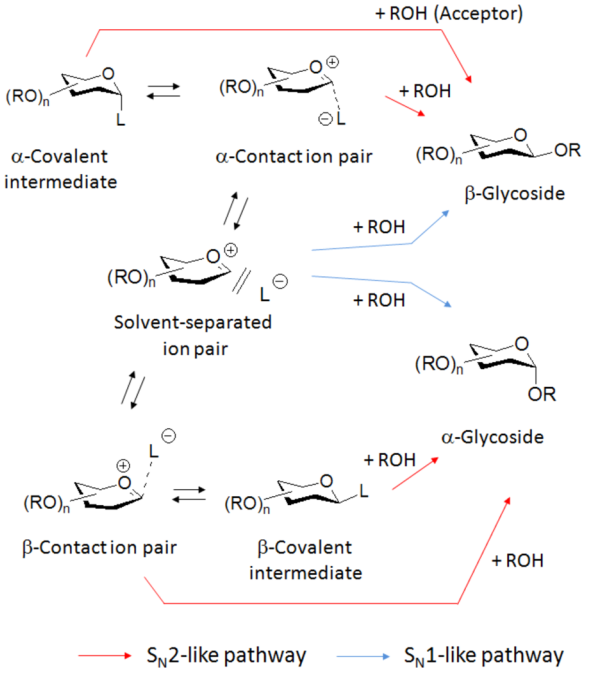

detailed reaction pathways have not been discussed with both the cationic glycosyl part and the anionic leaving group being taken into consideration. On one hand, the model systems employed in the computation might have been not sufficiently experimentally relevant, and on the other hand the computational methods used were not suitable for calculating these ion pairs. These considerations strongly suggest that the system employed in the computation of glycosylation reaction must mimic the experimental systems as closely as possible to be of relevance for organic synthesis and also that the accuracy and predictive power of the computational methods must be carefully checked.

The present study is concerned with quantum chemical computations employing mainly 2,3,4,6-tetra-*O*-methyl-α-D-glucopyranosyl triflate (**CIα**) as a model glycosyl donor, aiming to prove the presence of the equilibrium in Scheme 1. As mentioned above, the triflate glycosyl donors are one of the most widely investigated covalent intermediates,[1b,c,4−10] and hence the computational results obtained can be easily compared to the experimental results reported previously. We discuss the performance of several theories by calculating the heterolytic bond dissociation energy of the glycosidic bond of **CIα** and subsequently address the chemical nature of the covalent intermediates and the ion pairs.

COMPUTATIONAL DETAILS

The GAUSSIAN 09 software was employed in these calculations.[26] Geometry optimization was carried out at the DFT level of theory with the M06-2X functional,[27] which was employed as it generally reproduces well the structures of organic molecules and correctly represents dispersion energies. The 6-31G(d,p) basis sets were employed for H, C, O, F, S, and Cl, with diffuse functions being added to O, F, and Cl. This basis set system is named BS-I. For energy evaluation, we employed the MP4(SDQ) method and the DFT methods with B3LYP,[28] mPW1PW91,[29] B3PW91,[30] PBE1PBE,[31] O3LYP,[32] and M06-2X functionals. In this case, a higher basis set system (BS-II) was used: 6-311G(d,p) with addition of diffuse functions to O, F, and Cl. We also employed a larger basis set (BS-III), with the aug-cc-pVTZ basis set for O, F, and Cl and cc-pVTZ for H, C, and S. In all calculations, the solvation energy in dichloromethane was evaluated according to the PCM method with the keyword of "SCRF" and the option of "PCM" being used. In the PCM calculation, the UFF parameters were used to determine the cavity size. It was ascertained that each equilibrium geometry exhibited no imaginary frequency and each transition state exhibited one imaginary frequency. The pyranosyl ring conformation of the optimized species was evaluated with the Cremer−Pople puckering parameter.[33]

Enthalpy, entropy, and Gibbs energy changes were calculated at 195.15 K (−78 °C), since this temperature is frequently employed in glycoside synthesis involving triflate donors. Zero-point energy, thermal energy, and entropy change were evaluated at the DFT-(M06-2X) level of theory. The translational entropy in dichloromethane was computationally treated according to the literature.[34]

RESULTS AND DISCUSSION

Evaluation of Computational Methods. We first optimized the geometry of the α-covalent intermediate **CIα** at the DFT(M06-2X) level of theory. The optimization produced the $^4C_1$ pyranosyl ring geometry with the C-1−OTf bond length being 1.484 Å, as shown in Figure 1. The

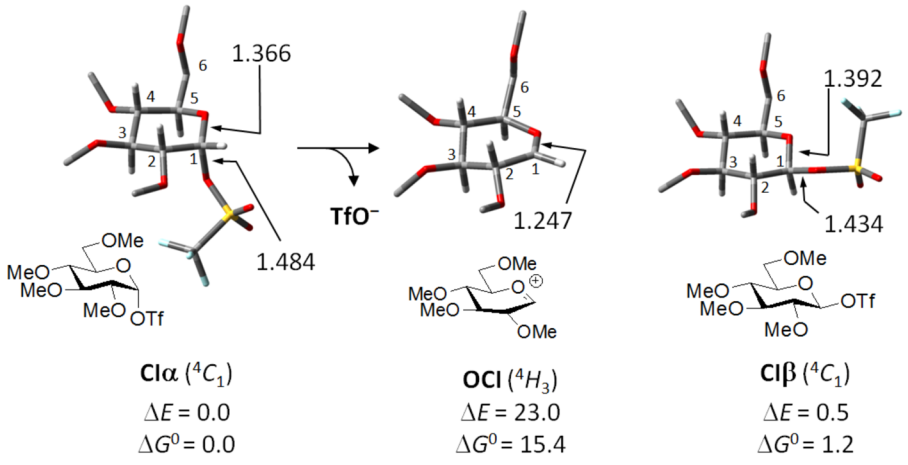

Figure 1. Geometries and relative energies (in kcal/mol) of the covalent intermediates **CIα** and **CIβ** and the oxacarbenium ion **OCI**, calculated at the DFT(M06-2X)/BS-III//DFT(M06-2X)/BS-I level with solvation in dichloromethane taken into account with the PCM method for both energy and geometry. The pyranosyl ring conformation is given in parentheses after the compound name.

dx.doi.org/10.1021/jo501012s | J. Org. Chem. 2014, 79, 7889−7894

optimized C-1−OTf bond is somewhat longer than a typical C−O bond: for example, the C−O bond of methanol was calculated to be 1.423 Å at the same computational level. The fact that the TfO group is an extremely good leaving group is probably due to this long C-1−OTf distance.

Geometry optimization of an oxacarbenium ion formed by an ionic C-1−OTf bond cleavage was then performed, affording the geometry **OCI** (Figure 1). The optimized geometry exhibited a $^4H_3$ ring conformation and a significantly shortened O-5−C-1 bond (to 1.247 Å from 1.366 Å in **CIα**). These geometrical values agree well with those reported for the oxacarbenium ion.[24] Several computational studies suggested the presence of other conformers of **OCI**, such as $^1C_4$ and E_3,[17,24] but we omit such minor conformations, as they are reported to be significantly less stable than **OCI** with the $^4H_3$ conformation. Note that we calculated only *gauche-gauche* (*gg*) hydroxymethyl rotamers for all chemical species in this study, as the *gg* rotamer is usually more stable than the other rotamers *gauche-trans* and *trans-gauche*;[35] see also Figure S1 in Supporting Information for a more detailed discussion.

The formation of the ion pairs from **CIα** always involves an ionic cleavage of the C-1−OTf bond. The computational method used for the simulation of the equilibrium in Scheme 1 thus has to correctly estimate the heterolytic bond dissociation energy (HBDE) of this bond. This HBDE represents the energy change along the reaction path producing the oxacarbenium ion **OCI** and the triflate anion TfO^- from **CIα**, as shown in Figure 1. To this end, we calculated the HBDE at several levels of theory. The HBDE on the basis of Gibbs energy ($\Delta G°$) was calculated to be 15.4 kcal/mol at the MP4(SDQ)//DFT(M06-2X) level of theory, the zero-point corrected potential energy change (ΔE) being 23.0 kcal/mol (Figure 1).[36] The ΔE value converges upon going from MP2 to MP4(SDQ), as given in Table 1. The MP4(SDQ) energies are thus the most reliable—provided of course that the energy converges—as the MP4(SDQ) method usually provides energies of very high accuracy, especially in the case of ionic reactions.

Table 1. Zero-Point-Corrected Potential Energy Changes (ΔE, in kcal/mol) in the C-1−OTf Bond Dissociation of CIα Calculated at Various Levels of Theory

computational method	ΔE^a
MP2/BS-II	25.3
MP3/BS-II	24.5
MP4(DQ)/BS-II	23.0
MP4(SDQ)/BS-II	23.0
DFT(M06-2X)/BS-II	25.4
DFT(M06-2X)/BS-III	22.1
DFT(B3LYP)/BS-II	8.3
DFT(B3PW91)/BS-II	10.8
DFT(mPW1PW91)/BS-II	14.2
DFT(PBE1PBE)/BS-II	16.7
DFT(O3LYP)/BS-II	1.9

[a]Zero-point correction for potential energy was made at the DFT(M06-2X) level.

Considering the complexity of the donor, acceptor, and solvent molecules to be simulated, the MP4(SDQ) method is not a realistic choice from the viewpoint of computational cost. We thus decided to scrutinize DFT functionals, looking for one that yields a potential energy similar to that of the MP4(SDQ) method.[37] As shown in Table 1, the zero-point corrected potential energy change (ΔE) at the DFT(M06-2X)/BS-III level (22.1 kcal/mol) is the closest to the MP4(SDQ)-calculated value, whereas the other DFT functionals considerably underestimated the energy change. We therefore selected the DFT(M06-2X)/BS-III method for the energy evaluation of the covalent intermediate and the ion pairs.[38] Another advantage of the M06-2X functional is that it is reasonably correct with regard to dispersion forces, while the others tend to be relatively poor at representing those weak interactions.[27]

Equilibrium between Covalent Intermediates and Ion Pairs. As the next step, geometry optimization of a β-covalent intermediate **CIβ**, the C-1 epimer of **CIα**, was carried out at the DFT(M06-2X) level. As shown in Figure 1, the geometry of **CIβ** was successfully optimized with the $^4C_1$ ring conformation and the C1−OTf bond length being 1.434 Å. The Gibbs energy ($\Delta G°$) of **CIβ** was 1.2 kcal/mol higher than that of **CIα**, which agrees with the experimental fact that only α-triflate was observable in low-temperature NMR experiments. We then attempted to optimize the geometries of the contact ion pairs and the solvent-separated ion pairs, starting from geometries with elongated C-1−OTf bonds. The geometry optimization of the ion pairs, however, was not successful, ending up in re-formation of either **CIα** or **CIβ**. Computations on a similar glycosyl triflate by Whitfield showed that such ion pairs could exist as equilibrium species if a lithium cation was added close to TfO^- to balance the negative charge concentrated on the O atoms.[18] That report agrees well with our current results.

In the following, we attempt to perform geometry optimization with four explicit solvent molecules taken into account. We employed dichloromethane as the solvent, since it is one of the most common solvents utilized in glycoside synthesis. For the position of the solvent molecules in the starting geometry, we placed three dichloromethane molecules close to the three O atoms of the TfO moiety and one dichloromethane molecule on one side of the donor opposite to the location of the TfO group. The C−H moiety of dichloromethane will act as a negative charge balance for TfO^-, as the lithium cation did in the studies by Whitfield,[18] and the Cl atoms of dichloromethane will also significantly stabilize the C-1 cationic center, overall rendering the ion pairs stable enough to exist as equilibrium species. The above problem, the re-formation of **CIα** and **CIβ** upon geometry optimization of the ion pairs, was solved by the presence of the solvent molecules. Thus, the optimized geometries of the α-contact ion pair **CIPα**, the β-contact ion pair **CIPβ**, and six solvent-separated ion pairs are shown in Figures 2−4.

These ion pairs have ring conformations similar to that of **OCI** ($^4H_3$) with short O-5−C-1 bonds, indicating that the glycosyl part of these ion pairs has a chemical nature similar to that of **OCI** and accordingly the TfO^- group also has an anionic nature. In the contact ion pairs, the C-1−OTf bond is greatly elongated, with lengths of 2.371 and 2.464 Å for **CIPα** and **CIPβ**, respectively, but there is no solvent molecule separating the oxacarbenium ion and TfO^- (Figures 2 and 3). In case of the solvent-separated ion pairs, in contrast, at least one solvent molecule separates the cationic and the anionic parts. In **SSIP1**, for example, two molecules of dichloromethane stabilize the cationic C-1 center from both the α- and β-faces, pushing TfO^- away from C-1 of the oxacarbenium ion (Figure 4). It is likely that these solvent-separated ion pairs are in

dx.doi.org/10.1021/jo501012s | J. Org. Chem. 2014, 79, 7889−7894

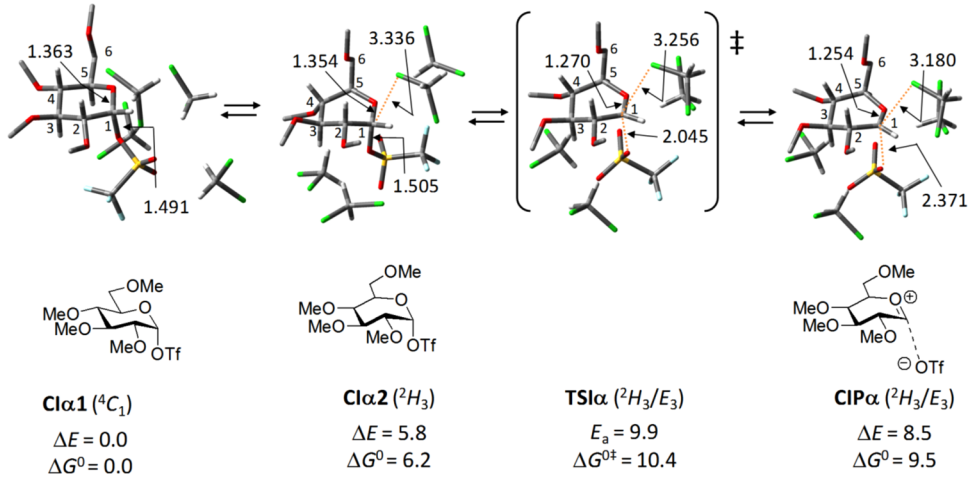

Figure 2. Geometry changes and energy profile of the reaction from the α-covalent intermediate **ClI*α*** to the contact ion pair **ClP*α***. The computation was performed at the DFT(M06-2X) level with four explicit solvent molecules of dichloromethane taken into account. The hydrogen atoms of the methyl protecting groups and the sixth carbon of the donor are not shown. Bond lengths and energies are given in Å and kcal/mol, respectively. The pyranosyl ring conformation is given in parentheses after the compound name.

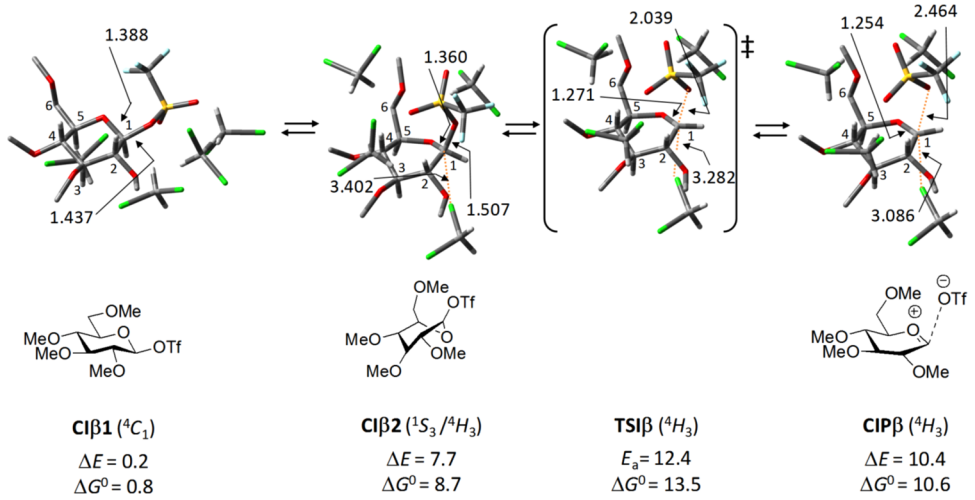

Figure 3. Geometry changes and energy profile of the reaction from the β-covalent intermediate **ClI*β*** to the β-contact ion pair **ClP*β***. The computation was performed at the DFT(M06-2X) level with four explicit solvent molecules of dichloromethane taken into account. The hydrogen atoms of the methyl protecting groups and the sixth carbon of the donor are not shown. Bond lengths are given in Å. The energy in kcal/mol is taken relative to the most stable **ClI*α*1**; see Figure 1. The pyranosyl ring conformation is given in parentheses after the compound name.

equilibrium, judging from their similar Gibbs energies, although detailed transitions between them were not investigated.

In addition, the transition states connecting the covalent intermediates to the ion pairs are displayed in Figures 2 and 3: **TSI*α*** for the transition from **ClI*α*** to **ClP*α*** and **TSI*β*** for the transition from **ClI*β*** to **ClP*β***. The formation of the contact ion pairs starts from pyranosyl ring conformations different from the most stable $^4C_1$: **ClP*α*** from a $^2H_3$ conformer and **ClP*β*** from a $^1S_3/^4H_3$ conformer. This conformational change will easily occur also at low temperatures, such as −78 °C, since activation barriers for the conformational conversion of the pyranosyl ring are generally sufficiently small: 5−15 kcal/mol.[39] The activation Gibbs energies ($\Delta G^{\circ\ddagger}$) for **TSI*α*** and **TSI*β*** for the formation of the contact ion pairs are thus more important than those for the conformational changes. The $\Delta G^{\circ\ddagger}$ values for **TSI*α*** and **TSI*β*** were calculated at the DFT(M06-2X) level to be 10.4−13.5 kcal/mol, respectively. These small $\Delta G^{\circ\ddagger}$ values are consistent with the reported experimental fact that the interconversion between the α- and β-covalent intermediates does occur at the low temperature of −78 °C.[1b,c] We did not investigate transitions between the contact ion pairs and the solvent-separated ion pairs, but they are certainly in equilibrium, as the six solvent-separated ion pairs have Gibbs energies similar to those of the contact ion pairs, regardless of whether the TfO^- anion is located on the α- or β-face (Figure 4). The dependence of the energy of the covalent intermediates and the ion pairs on the number of the solvent (dichloromethane) molecules taken into account was also studied: generally, four solvent molecules were sufficient to correctly represent the energy of the chemical species involved (see Figure S2 in the Supporting Information and the discussion there). In this study, the thermal movement of the solvent molecules is not accurately taken into account, although thermodynamic data from the frequency calculation qualitatively incorporate the effect derived from such fluctuation. In reality, however, the fluctuation of the solvent molecules plays a significant role in the reaction, and hence further studies should

dx.doi.org/10.1021/jo501012s | J. Org. Chem. 2014, 79, 7889−7894

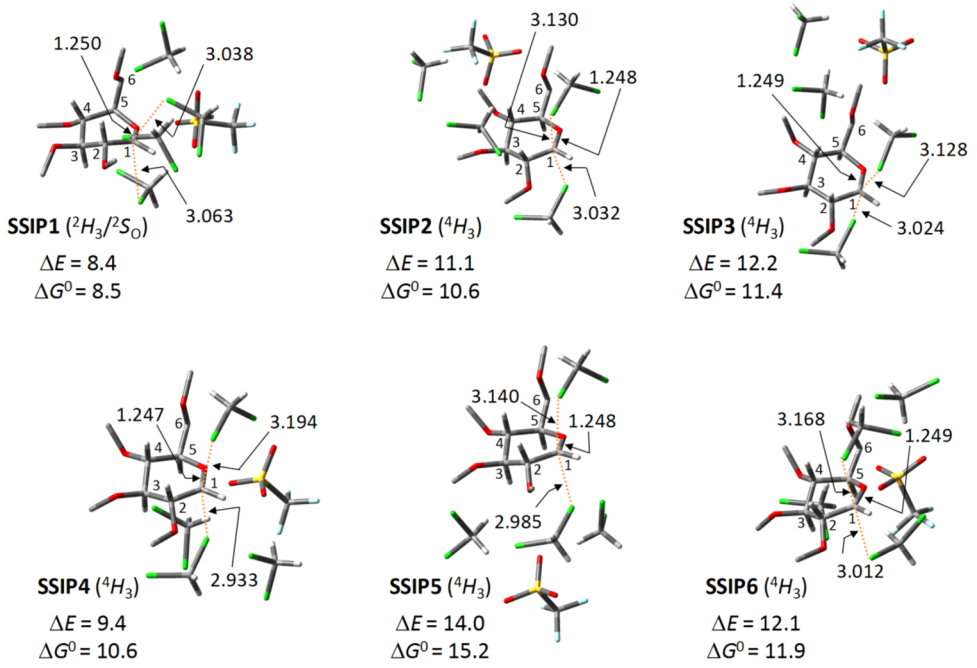

Figure 4. Optimized geometries of the solvent-separated ion pairs, computed at the DFT(M06-2X) level with four explicit solvent molecules of dichloromethane taken into account. The hydrogen atoms of the methyl protecting groups and the sixth carbon of the donor are not shown. Bond lengths are given in Å. The energy in kcal/mol is taken relative to the most stable **CIα1**; see Figure 1. The pyranosyl ring conformation is given in parentheses after the compound name.

be done to get a closer approach to the role of the solvent molecules.

As frequently mentioned in previous works, oxacarbenium ions can adopt several pyranosyl ring conformations. $^4H_3$, $^3H_4$, $^5S_1$, and E_3 conformations have been identified as important ones for glycosylation reactions.[5,23,24] It is therefore pivotal to discuss the dependence of the stability of the ion pairs on the pyranosyl ring conformations. However, methods for a thorough conformational search such as ab initio molecular dynamics are obviously inapplicable, as the system we employed is very large. We instead performed geometry optimization of the contact ion pairs and the solvent-separated ion pairs starting from the four ring conformations presented above, with the same solvent configurations as in **CIPα**, **CIPβ**, and **SSIP1** (Figures 2−4). Optimization of the α-contact ion pair resulted in the re-formation of **CIα** with the $^2H_3/E_3$ conformation (see Figure 2), no matter from which conformation, $^4H_3$, $^3H_4$, $^5S_1$, or E_3, the geometry optimization started (see Table S1 in the Supporting Information for more details). This suggests the conformational changes in the α-contact ion pair to be highly restricted. For the β-contact ion pair, on the other hand, several stable conformations, $^4H_3$, $^{2,5}B$, and $B_{2,5}$, were found, $^4H_3$ (**CIPβ** in Figure 3) being the most stable. Also, $^2H_3/^2S_0$, $^{2,5}B$, and E_3 conformers were optimized for the solvent-separated ion pair, and $^2H_3/^2S_0$ (**SSIP1** in Figure 4) was the most stable. Thus, relatively flexible conformational changes can occur in the case of the β-contact ion pair and the solvent-separated ion pair (see also Figure S4 in the Supporting Information for the optimized geometries other than those in Figures 2−4).[40] All of these results strongly suggest that the oxacarbenium ion conformation is strongly influenced by the position of the counteranion. For an accurate simulation of glycosylation reactions, it is therefore indispensable that the counteranion and solvent molecules be explicitly taken into account.

CONCLUSIONS

We carried out quantum chemical computations to investigate the equilibrium among the covalent intermediates, the contact ion pairs, and the solvent-separated ion pairs in a typical glycosidation reaction. We first screened DFT functionals for good applicability to the reaction system and found that the M06-2X functional gave results similar to those at the most accurate MP4(SDQ) level. The geometries of the ion pairs were successfully optimized only when several solvent (dichloromethane) molecules were explicitly involved. The calculated $\Delta G^{\circ\ddagger}$ value of several transitions in the equilibrium were considerably low (10.4−13.5 kcal/mol), and hence the equilibrium can be achieved at very low temperatures. These ion pairs take several pyranosyl ring conformations, and the stability of the conformers is highly dependent on the relative position of the counterion.

The present study is the first to provide theoretical proof for the presence of an equilibrium between the covalent intermediates and the ion pairs in glycoside synthesis. Further investigation on the reactivity of the covalent intermediates and the ion pairs toward glycosyl acceptors will clarify the overall reaction paths in chemical glycoside synthesis.

ASSOCIATED CONTENT

Supporting Information

Text, figures, and tables giving the energies of the *gt*-hydroxymethyl rotamers of the α-covalent triflate **R** and the oxacarbenium ion **OCI** (Figure S1), geometries and potential energies of the α-covalent intermediates and the ion pairs with one to four solvent molecules taken into account (Figure S2), changes in pyranosyl ring conformation during geometry optimization starting from various conformers, along with the Gibbs energies of the optimized geometries (Table S1), geometries of the α-contact ion pair, the β-contact ion pair, and the solvent-separated ion pair before and after the

dx.doi.org/10.1021/jo501012s | J. Org. Chem. 2014, 79, 7889−7894

optimization staring from various pyranosyl ring conformations (Figure 3A–C), geometries of the ion pairs that are not shown in Figures 2–4 in the text (Figure S4), and Cartesian coordinates of the optimized geometries. This material is available free of charge via the Internet at http://pubs.acs.org.

AUTHOR INFORMATION

Corresponding Author

*E-mail for T.H.: takashi.hosoya@boku.ac.at

Notes

The authors declare no competing financial interest.

ACKNOWLEDGMENTS

We performed quantum chemical calculations with the workstation in the Sakaki group, Fukui institute for fundamental chemistry at Kyoto University, Kyoto, Japan, and wish to thank them for the access. The financial support of the Austrian Christian Doppler Research Society (CDG) through the CD-lab "Advanced cellulose chemistry and analytics" is gratefully acknowledged.

REFERENCES

(1) Recent reviews for chemical glycoside synthesis: (a) Walvoort, M. T. C.; van der Marel, G. A.; Overkleeft, H. S.; Codée, J. D. C. *Chem. Sci.* **2013**, *4*, 897–906. (b) Crich, D. *Acc. Chem. Res.* **2010**, *43*, 1144–1153. (c) Crich, D. *J. Org. Chem.* **2011**, *76*, 9193–9209. (d) Zhu, X.; Schmidt, R. R. *Angew. Chem., Int. Ed.* **2009**, *48*, 1900–1934. (e) Walvoort, M. T. C.; Dinkelaar, J.; van den Bos, L. J.; Lodder, G.; Overkleeft, H. S.; Codée, J. D. C.; van der Marel, G. A. *Carbohydr. Res.* **2010**, *345*, 1252–1263.

(2) Koenigs, W.; Knorr, E. *Ber. Dtsch. Chem. Ges.* **1901**, *34*, 957–981.

(3) Ngoje, G.; Li, Z. *Org. Biomol. Chem.* **2013**, *11*, 1879–1886.

(4) Huang, M.; Garrett, G. E.; Birlirakis, N.; Bohé, L.; Pratt, D. A.; Crich, D. *Nat. Chem.* **2013**, *4*, 663–667.

(5) Dinkelaar, J.; de Jong, A. R.; van Meer, R.; Somers, M.; Lodder, G.; Overkleeft, H. S.; Codée, J. D. C.; van der Marel, G. A. *J. Org. Chem.* **2009**, *74*, 4982–4991.

(6) Crich, D.; Vinogradova, O. *J. Org. Chem.* **2006**, *71*, 8473–8480.

(7) Crich, D.; de la Mora, M.; Vinod, A. U. *J. Org. Chem.* **2003**, *68*, 8142–8148.

(8) (a) Callam, C. S.; Gadikota, R. R.; Krein, D. M.; Lowary, T. L. *J. Am. Chem. Soc.* **2003**, *125*, 13112–13119. (b) Hou, D.; Taha, H. A.; Lowary, T. L. *J. Am. Chem. Soc.* **2009**, *131*, 12937–12948.

(9) Huang, M.; Retailleau, P.; Bohé, L.; Crich, D. *J. Am. Chem. Soc.* **2012**, *134*, 14746–14749.

(10) Crich, D.; Sun, S. *J. Am. Chem. Soc.* **1997**, *119*, 11217–11223.

(11) Beaver, M. G.; Woerpel, K. A. *J. Org. Chem.* **2010**, *75*, 1107–1118.

(12) (a) Krumper, J. R.; Salamant, W. A.; Woerpel, K. A. *J. Org. Chem.* **2009**, *74*, 8039–8050. (b) Krumper, J. R.; Salamant, W. A.; Woerpel, K. A. *Org. Lett.* **2008**, *10*, 4907–4910.

(13) Jensen, H. H.; Nordstrøm, L. U.; Bols, M. *J. Am. Chem. Soc.* **2004**, *126*, 9205–9213.

(14) Lemieux, R. U.; Hendriks, K. B.; Stick, R. V.; James, K. *J. Am. Chem. Soc.* **1975**, *97*, 4056–4062.

(15) The presence of the equilibrium is indicated from the kinetic isotope effect and the cation clock methods: see refs 4 and 9.

(16) (a) Denekamp, C.; Sandlers, Y. *J. Mass Spectrom.* **2005**, *40*, 765–771. (b) Denekamp, C.; Sandlers, Y. *J. Mass Spectrom.* **2005**, *40*, 1055–1063.

(17) Whitfield, D. M. *Carbohydr. Res.* **2012**, *356*, 191–195.

(18) (a) Whitfield, D. M. *Carbohydr. Res.* **2012**, *356*, 180–190. (b) Whitfield, D. M. *Carbohydr. Res.* **2007**, *342*, 1726–1740.

(19) Kumar, R.; Whitfield, D. M. *J. Org. Chem.* **2012**, *77*, 3724–3739.

(20) Li, Z. *Carbohydr. Res.* **2010**, *345*, 1952–1957.

(21) Satoh, H.; Hansen, H. S.; Manabe, S.; van Gunsteren, W. F.; Hünenberger, P. H. *J. Chem. Theory Comput.* **2010**, *6*, 1783–1797.

(22) Ionescu, A. R.; Whitfield, D. M.; Zgierski, M. Z. *Carbohydr. Res.* **2007**, *342*, 2793–2800.

(23) Ionescu, A. R.; Whitfield, D. M.; Zgierski, M. Z.; Nukada, T. *Carbohydr. Res.* **2006**, *341*, 2912–2920.

(24) Nukada, T.; Bérces, A.; Wang, L.; Zgierski, M. Z.; Whitfield, D. M. *Carbohydr. Res.* **2005**, *340*, 841–852.

(25) Nukada, T.; Bérces, A.; Whitfield, D. M. *Carbohydr. Res.* **2002**, *337*, 765–774.

(26) Frisch, M. J.; Trucks, G. W.; Schlegel, H. B.; Scuseria, G. E.; Robb, M. A.; Cheeseman, J. R.; Scalmani, G.; Barone, V.; Mennucci, B.; Petersson, G. A.; Nakatsuji, H.; Caricato, M.; Li, X.; Hratchian, H. P.; Izmaylov, A. F.; Bloino, J.; Zheng, G.; Sonnenberg, J. L.; Hada, M.; Ehara, M.; Toyota, K.; Fukuda, R.; Hasegawa, J.; Ishida, M.; Nakajima, T.; Honda, Y.; Kitao, O.; Nakai, H.; Vreven, T.; Montgomery, J. A., Jr.; Peralta, J. E.; Ogliaro, F.; Bearpark, M.; Heyd, J. J.; Brothers, E.; Kudin, K. N.; Staroverov, V. N.; Kobayashi, R.; Normand, J.; Raghavachari, K.; Rendell, A.; Burant, J. C.; Iyengar, S. S.; Tomasi, J.; Cossi, M.; Rega, N.; Millam, N. J.; Klene, M.; Knox, J. E.; Cross, J. B.; Bakken, V.; Adamo, C.; Jaramillo, J.; Gomperts, R.; Stratmann, R. E.; Yazyev, O.; Austin, A. J.; Cammi, R.; Pomelli, C.; Ochterski, J. W.; Martin, R. L.; Morokuma, K.; Zakrzewski, V. G.; Voth, G. A.; Salvador, P.; Dannenberg, J. J.; Dapprich, S.; Daniels, A. D.; Farkas, Ö.; Foresman, J. B.; Ortiz, J. V.; Cioslowski, J.; Fox, D. J. *Gaussian 09, Revision D.01*; Gaussian, Inc., Wallingford, CT, 2009.

(27) Zhao, Y.; Truhlar, D. G. *Theor. Chem. Acc.* **2008**, *120*, 215–241.

(28) (a) Becke, A. D. *Phys. Rev. A* **1988**, *38*, 3098–3100. (b) Lee, C.; Yang, W.; Parr, R. G. *Phys. Rev. B* **1988**, *37*, 785–789. (c) Becke, A. D. *J. Chem. Phys.* **1993**, *98*, 5648–5652.

(29) Adamo, C.; Barone, V. *J. Chem. Phys.* **1998**, *108*, 664–675.

(30) (a) Perdew, J. P.; Chevary, J. A.; Vosko, S. H.; Jackson, K. A.; Pederson, M. R.; Singh, D. J.; Fiolhais, C. *Phys. Rev. B* **1992**, *46*, 6671–6687. (b) Perdew, J. P.; Chevary, J. A.; Vosko, S. H.; Jackson, K. A.; Pederson, M. R.; Singh, D. J.; Fiolhais, C. *Phys. Rev. B* **1993**, *48*, 4978. (c) Perdew, J. P.; Burke, K.; Wang, Y. *Phys. Rev. B* **1996**, *54*, 16533–16539.

(31) (a) Perdew, J. P.; Burke, K.; Ernzerhof, M. *Phys. Rev. Lett.* **1996**, *77*, 3865–3868. (b) Perdew, J. P.; Burke, K.; Ernzerhof, M. *Phys. Rev. Lett.* **1997**, *78*, 1396. (c) Adamo, C.; Barone, V. *J. Chem. Phys.* **1999**, *110*, 6158–6169.

(32) (a) Handy, N. C.; Cohen, A. J. *Mol. Phys.* **2001**, *99*, 403–412. (b) Cohen, A. J.; Handy, N. C. *Mol. Phys.* **2001**, *99*, 607–615.

(33) Cremer, D.; Pople, J. A. *J. Am. Chem. Soc.* **1975**, *97*, 1354–1358.

(34) Mammen, M.; Shakhnovich, E. I.; Deutch, J. M.; Whitesides, G. M. *J. Org. Chem.* **1998**, *63*, 3821–3830.

(35) See for example: Kirschner, K. N.; Woods, R. J. *Proc. Natl. Acad. Sci. U.S.A.* **2001**, *98*, 10541–10545.

(36) ΔG° is significantly lower than ΔE because of an increase in entropy by the C-1–OTf cleavage. Note that the decrease in entropy by the rearrangement of the solvent before and after the ionic cleavage is indirectly incorporated in the evaluation of the solvation energy with the PCM method.

(37) As discussed later, taking solvent molecules explicitly into account is necessary for an accurate simulation of the ion pair formation. However, the simplified system taken here should be sufficient for the evaluation of the DFT functionals.

(38) A study scrutinizing DFT functionals also recommends the M06-2X functional as one of the most accurate functionals: Zheng, J.; Zhao, Y.; Truhlar, D. G. *J. Chem. Theory Comput.* **2009**, *5*, 808–821.

(39) See for example: Biarnés, X.; Ardèvol, A.; Planas, A.; Rovira, C.; Laio, A.; Parrinello, M. *J. Am. Chem. Soc.* **2007**, *129*, 10686–10693.

(40) The energy barrier for the conformational change of the ion pair is expected to be sufficiently small in most cases to allow conformational changes of the pyranosyl ring, according to an ab initio molecular dynamics study carried out for several oxacarbenium ions; see ref 23.